Estudio de la dinámica de la submarea invernal en la ensenada del sur de Brasil mediante un modelo barotrópico de circulación

José L. Stech and João A. Lorenzzeti
National Institute for Space Research
Division of Earth Sciences
São José dos Campos, S.P., C.P. 515. Brazil

RESUMEN

En este trabajo se utiliza un modelo numérico barotrópico de una capa, formulado en elementos finitos, para estudiar la circulación asociada a la submarea invernal en la plataforma continental del sureste brasileño. En concreto se determina la respuesta de las aguas continentales al efecto del viento en dos casos: a) con vientos variables en espacio y tiempo, obtenidos de un modelo conceptual de frentes fríos; y b) con un campo de vientos derivado de observaciones en estaciones costeras y mapas sinópticos. Los resultados de estos experimentos se utilizaron para determinar los balances de vorticidad y cantidad de movimiento dominante. Asimismo, con objeto de analizar la aparición de ondas cuasi-inerciales se desarrolló un modelo simplificado de resonancia. Finalmente, para explicar la propagación de las señales de niveles anómalos del mar se realizaron análisis de correlación de tales anomalías entre varios puntos a lo largo de la costa y de la dispersión de las olas en aguas continentales libres.

The subtidal wintertime dynamics of the South Brazilian Bight as seen through a barotropic circulation model

José L. Stech and João A. Lorenzzeti
National Institute for Space Research
Division of Earth Sciences
São José dos Campos, S.P., C.P. 515. Brazil

ABSTRACT

The winter time subtidal circulation dynamics of the southeast continental shelf of Brazil are studied using a one-layer barotropic numerical model formulated in finite elements. The response of the shelf waters to the wind forcing was studied for two cases: a) variable temporal and spatial wind, obtained from a conceptual model of cold fronts; and b) a wind field obtained from coastal stations and synoptic charts. The results from these experiments were used to determine the dominant momentum and vorticity balances. A simplified resonance model was developed to explain the appearance of quasi-inertial waves. Correlation analysis of sea level anomalies between various points along the coast and the dispersion relation of free continental shelf waves were used to explain the propagation of the sea level anomaly signals present in the numerical results.

1. INTRODUCTION

Although sometimes considered as only a specialization of the methods employed in large scale physical oceanography, the study of the processes of oceanic circulation over the continental shelves has its own pecularities. For example, the small depths (i.e., 0 - 200 m) observed in these regions make both the bottom topographic effect and the bottom friction very important, in great contrast to the deep ocean. Also, the proximity of the coast is a strong constraint on the flow, with the result that the cros-shore flow becomes negligible as the coastline is approached. This effect, together with the fact that the shelf width is much smaller than its alongshore dimension, also results in a predominantly alongshelf flow. Similar to the deep ocean, the effects of rotation (Coriolis acceleration) cannot be neglected for continental

Física de la Tierra, núm. 3. 283-306. Ed. Univ. Compl. Madrid, 1991.

shelves, due to great alongshelf dimension for most of these regions (100 1.000 km) and the time scales from days to weeks for energetic events.

In general, three approachs can be used for the study of the dynamics of the continental shelves: a) field work for the collection of an extensive data set, including current meter moorings, sea level gauges, hydrographic stations, and meteorological measurements; b) analytical studies envolving the solution of some simplified version of the hydrodynamic equations of motion; and c) numerical modelling. The first approach is always desirable, but the high costs and the complex logistics involved are an impeding factor in most cases. Analytical studies are of great use in providing the basic theoretical background for interpreting the results of both numerical models and field work. Their limitations are associated with the many simplifications made in the equations in order to obtain a mathematically tractable problem.

At present, the availability of computer resources of great capacity with moderate costs, has made numerical modelling approach a very efficient tool, for the study of continental shelf processes. One of the main advantages of this technique is the ease of using the full set of hydrodynamic equations, and of incorporating the real bottom topography and coastline geometry, which results in much more realistic boundary conditions.

It should be noted, however, that the choice of the tecnique of numerical modelling also allows some simplifications be made for specific applications. For example, during the winter season the mixed layer over the continental shelf is generally well developed, with the water column showing only small vertical variations in temperature and salinity. For this situation, the use of one-layer, barotropic two-dimensional numerical models have produced in many cases satisfactory results in the description of the coastal circulation (e.g. Kourafalou *et al.*, 1984).

For the summer season, the increase in solar radiation and the weakening of the surface wind speed result an increase in the vertical stratification over the water column. In such cases, multi-layer baroclinic models are necessary for an adequate representation of the vertical shears present (Leendertse *et al.*, 1975, Signorini, 1979). For cases where a well developed pycnocline is present, acting as a material interface separating two fluids of different densities, satisfactory results can be obtained using two-layer models to study coastal circulation (Lorenzzetti *et al.*, 1988).

The South Brazilian Bight (SSB) is defined as the southeastern continental shelf region of Brazil, extending from Cabo de São Tomé (lat. 22° 00'S, long. 41° 00'W) to Cabo de Santa Marta (lat. 28° 37'S, long. 48° 49'W) Castro Filho (1985). The bottom topography is very smooth with the isobaths tending to follow the coastline; the shelf break is located between the 150-200 m isobaths. The shelf width varies between 70 km in front Cabo Frio, to 200 km in front of Santos, in the central part of this shelf region (fig. 1).

Analysis of hydrographic data collected in this region shows that for the summer season, the water column is predominantly stratified in a two-layer mode, with a strong thermocline located 25-35 m beneath the surface. During the winter, the waters assume a weak vertical stratification for the inner and

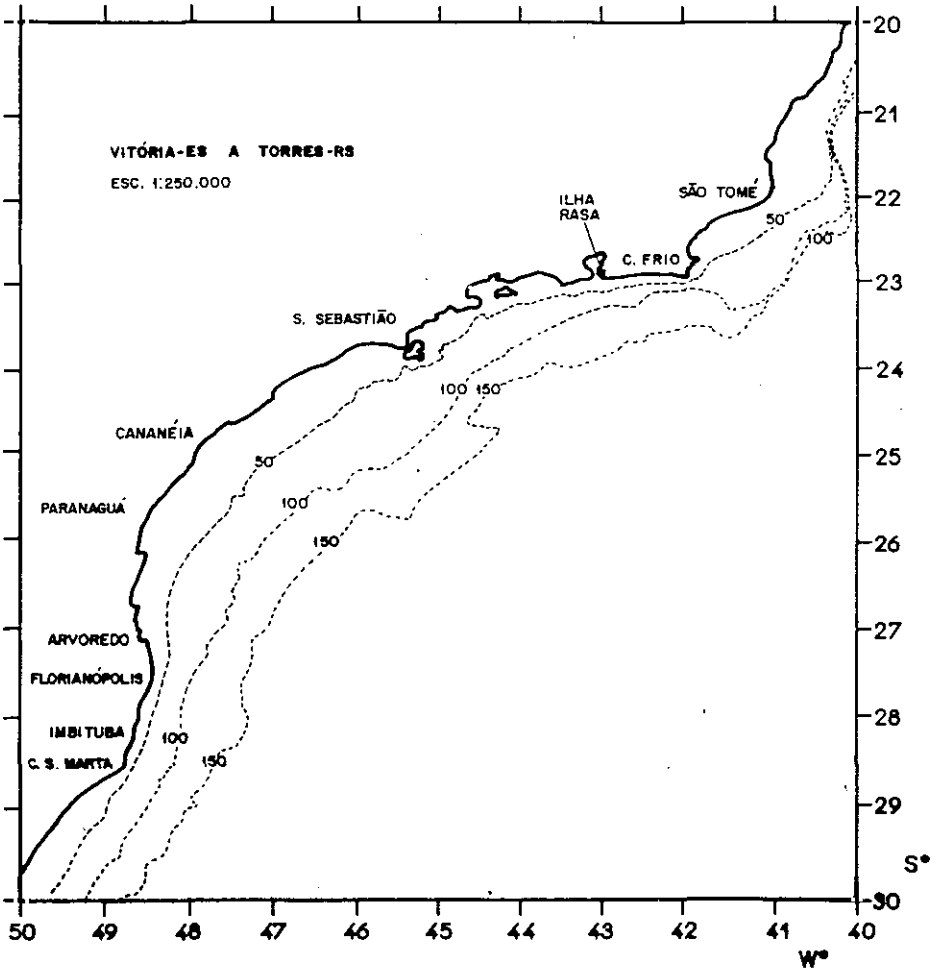

Figure 1.—Map of the South Brazilian Bight (SBB) with isobaths (dashed lines) in meters. The tidal and meteorological station positions referred to in the text are indicated by respective names.

mid-shelf regions; a noteciable stratification is present throughout the year near the shelf break due to inshore intrusions of Brazil Current Waters (Matsuura, 1983; Miranda, 1982; Castro Filho, 1985; Castro Filho *et al.*, 1987).

Thus, the hydrographic data collected in the SBB indicate that for the winter time, the implementation of a barotropic circulation model could be used to describe the main dynamical characteristics of the region. Therefore, with these arguments in mind, a one-layer barotropic numerical model, using the technique of finite elements is implemented for the region with the

purpose of studying its winter time circulation. The focus of this study is to provide a better understanding of the response of these shelf waters to wind forcing in the low frequency subtidal band.

2. DATA DESCRIPTIONN, PROCESSING AND ANALYSIS

2.1. Data Description

The surface wind data used in this study were collected at 0, 6, 12, 18 hours (local time) during the southern hemisphere winter (Jul/Aug/Sep), for the years 1980-1985, at the following coastal meteorological stations: Santa Marta, Arvoredo, Ilha Rasa and São Tomé (fig. 1). Geostrophic wind data, obtained from surface synoptic weather charts, were used to fill the missing wind data.

Infrared images from the GOES-W satellite were used with the purpose of analysing the pattern of propagation, the frequency of cold front penetration in the region and to verify the consistency of the wind data collected by the coastal stations.

Coastal sea level data were obtained from the following tidal gauge stations: Imbituba, Paranaguá, Cananéia, Rio de Janeiro and Cabo Frio areas (fig. 1). Atmospheric surface pressure, used to correct the low frequency barometric effect on the sea level data, were also collected at these meteorological stations.

2.2. Data processing

Several interpolation techniques were tested in order to fill the gaps in the time series of all the data sets. Each technique was tested by introducing artificial gaps in good portions of several of the time series and comparing the interpolated results againts the original data. The best overall results were obtained with the linear interpolation. It is speculated that the higher order interpolation tecniques did not produce good results due to the strong content of high frecuency energy present in the data. After the interpolation procedure, all time series were filtered, using a 40 hour low-pass Lanczos square digital filter (Walter and Heston, 1972) in order to remove high frequency energy in the data.

2.3. Data analysis

Stick plots of the wind vectors collected at the coastal meteorological stations for the winter of 1984, are shown in figure 2. It can be observed that the dominant winds are from northeast/north, varying to southwest/south with the penetration of the cold fronts in the region. In general, the strongest

winds tend to be found in the southern part of the domain. In the central part of the region, a marked weakening of the wind was observed. This effect is probably caused by the orographic effects of the Serra do Mar, a mountain range on the order of 700 m high, adjacent to the coast. This effect is particulary strong at the Moela coastal station, located between Cananéia and São Sebastião. For this reason, the wind data collected at this station were omitted from this study.

In order to fill the gap in the wind data for the central part of the domain, synoptic meteorological charts were used to derive the geostrophic wind which was then corrected to its surface value by the simplified model of atmospheric boundary layer given by Hasse (1974).

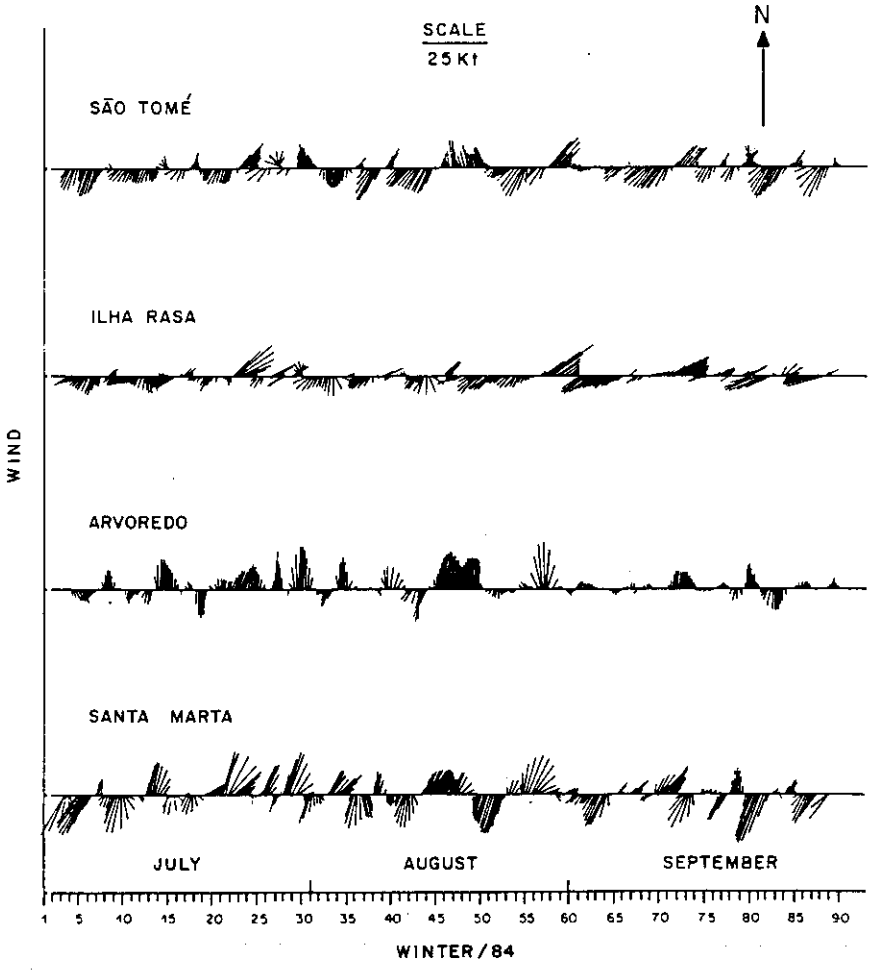

Figure 2. Low-pass filtered surface winds at Santa Marta, Arvoredo, Ilha Rasa and Cabo Frio for the winter of 1984.

To track the penetration and displacement of cold fronts in the region, the cloud field present in the infrared images of the GOES-W satellite was visually analysed for 0, 12, 18 and 21 hours GMT, for the years 1980-1985. The images were obtained by the National Institute for Space Research (INPE). This analysis revealed that the fronts tend to propagate in the alongshore direction, from southwest to northeast, with a mean time of 2 days for a particular front to cross the whole region. This corresponds, therefore, to a mean velocity of 500 km day^{-1}. It was also observed that aproximately 15 % of the cold fronts, penetrating the southern part of the domain, veer offshore and do not reach the Cabo Frio region. Upper level cyclonic vortices, which produce a strong increase in cloudness and precipitation in the region, were also detected in satellite images. On the average, this visual analysis showed that a cold front enters the region every 6 days. A summary of this analysis is given in Table I.

TABLE I

Statistics of winter time cold front penetrations on the southeast Brazilian coast derived from analysis of IR images of GOES-W sattellite. Results for 1984 are anomalous due to missing data for the month of august caused by problems in the sattellite.

Year	*Fronts in Sta. Marta*	*Fronts in S. Tomé*	*Mean Time between 2 Fronts (days)*	*Lag between Sta. Marta São Tomé (days)*	*Atmosph. Vortices*
1980	16	15	5.5	2.0	3
1981	11	10	6.9	2.1	2
1982	13	11	6.1	1.8	2
1983	13	11	6.2	1.9	—
1984*	8	7	6.3	1.9	4
1985	13	11	6.6	1.8	7

The time/space correlation of the wind between two different coastal stations was determined from the vector correlation technique of Kundu (1976). This method allows the determination of the lagged linear correlation between two vectorial time series with the results being independent of the orientation of the coordinate system used to decompose the wind vector. Table II shows the results of this analysis for the winter months of 1984 using the Santa Marta station as the reference.

The results in Table II show that the lag corresponding to a maximum correlation increases from 6 hours between Santa Marta and Arvoredo, to 42 hours between Santa Marta and São Tomé at the extreme north of the domain. This gradual increase of lag is consistent with the alongshore propagation of cold fronts previously described. A relatively high degree of wind correlation on the order of 0.70 is observed for the whole area.

TABLE II

Vector lagged correlation coefficients between the winds at Santa Marta and Arvoredo, Ilha Rasa and São Tomé stations (fig. 1).

Lag	*Lagged Correlation Coefficient*		
(hours)	*Sta. Marta Arvoredo*	*Sta. Marta Ilha Rasa*	*Sta. Marta São Tomé*
0	0.64	0.39	0.20
6	0.75	0.45	0.28
12	0.73	0.51	0.37
18	0.71	0.57	0.44
24	0.60	0.64	0.51
30	0.40	0.75	0.58
36	0.37	0.50	0.67
42	0.26	0.38	0.70

Main periodicities present in the wind data were determined through spectral analysis of the scalar time series of the rotated wind components (Jenkins and Watts, 1986). For each station, rotation was done to project the wind vector into the normal and parallel directions to the local coastline. The energy spectra, of both wind components for the Santa Marta station for 1984, are presented in figure 3.

The spectra of both components are dominated by an energy peak at the period of about 6 days; this is the characteristic period of the cold front penetration indicated in Table I. Most of the fluctuation energy is present in the alongshore component, due to the predominant orientation of the wind in that direction. Wind spectra for the other stations (not shown) are similar to that of Santa Marta.

3. A CONCEPTUAL MODEL OF COLD FRONTS FOR THE SBB

The analysis of synoptic charts, of satellite images and of coastal wind data has shown that in the mean, during the winter season, the cold fronts which penetrate the south part of Brazil propagate from southwest to northeast; the mean time of 2 days for the fronts to propagate through the region results in an average speed of 500 km day^{-1} for these systems. In the warm sector of the front the mean wind speed is 5 m s^{-1} and it rotates counterclockwise from its dominant northeast direction to northwest with the approaching of the front. In the cold sector, the mean wind speed is 8 m s^{-1}, rotating counterclockwise from southwest to northeast approximately 1 day after the passage of the front.

With these results in mind, a conceptual model of winter time cold fronts for the SBB was developed. This conceptual model is a time dependent and

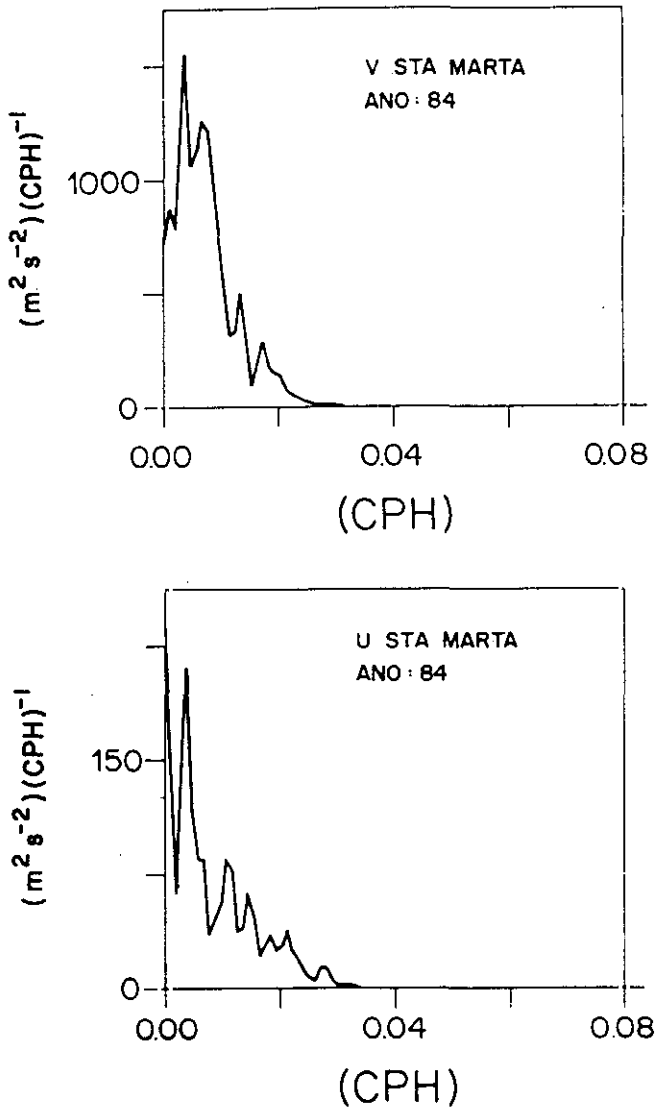

Figure 3.—Spectral energy density of the cross-shelf (U) and alongshelf (V) wind components for the winter of 1984 at Santa Marta station. The units are $m^2\ s^{-2}$ per cycle per hour.

space variable field of wind vectors containing the basic and more important characteristics of the real wind field associated with the frontal passages. A schematic representation of such model is shown in figure 4. The response of the SBB to cold front passages is then studied by using this conceptual model to force the barotropic circulation model.

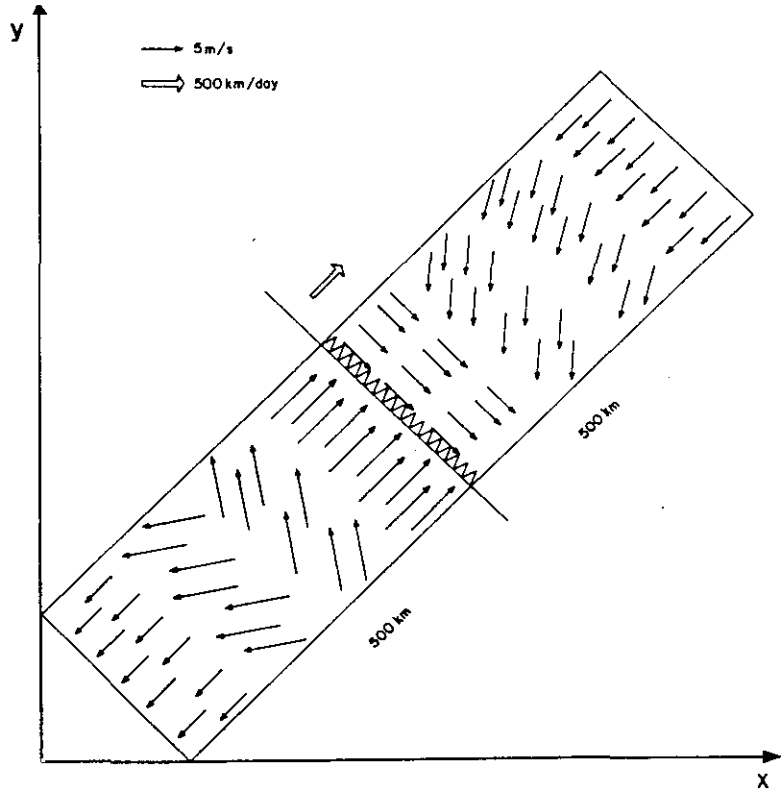

Figure 4.—A graphic representation of the Conceptual Model of cold fronts for the Southeast Brazil Region.

4. THE NUMERICAL MODEL

The model used in this investigation was formulated by Wang and Connor (1975), and is a one-layer barotropic two dimensional model, in which the Finite Element technique is used to solve the dynamical equations of motion. The equations used are the Navier-Stokes for the conservation of momentum and an equation of continuity for the conservation of mass to a fluid in rotation. The coordinate system is cartesian, has its origin at the ocean surface and the x, y, and z directions point to east, north and vertically upwards, respectively. The bottom topography is a function of x and y coordinates. The fluid system consists of one layer of constant density. The vertical acceleration is neglected in the vertical equation of momentum by the hydrostatic approximation. The vertical component of the Coriolis force is neglected. The Coriolis parameter is assumed constant throughout the region.

The following system of equations is obtained by the vertical integration of the equations of momentum and continuity from the bottom, to the free surface,

$$\frac{\partial q_x}{\partial t} + \frac{\partial u q_x}{\partial x} + \frac{\partial v q_x}{\partial y} = -gH \frac{\partial \eta}{\partial x} + \frac{1}{\rho}(\tau_{xs} - \tau_{xb}) + f q_y + F_x \tag{4.1}$$

$$\frac{\partial q_y}{\partial t} + \frac{\partial u q_y}{\partial x} + \frac{\partial v q_y}{\partial y} = -gH \frac{\partial \eta}{\partial y} + \frac{1}{\rho}(\tau_{ys} - \tau_{yb}) - f q_x + F_y \tag{4.2}$$

$$\frac{\partial \eta}{\partial t} + \frac{\partial q_x}{\partial x} + \frac{\partial q_y}{\partial y} = 0 \tag{4.3}$$

where, q_x and q_y represent the integrated transport per unit width in the x and y directions; u and v are the velocity components; η is the free surface anomalies; ρ is the water density; τ_{xs} and τ_{ys} are the wind stresses, and τ_{xb} and τ_{yb} are the bottom stresses. The wind and bottom stresses are both parameterized using quadratic formulation as follows:

$$\vec{\tau}_s = \rho_{\text{air}} C_w |\vec{U}_{10}| \vec{U}_{10} \tag{4.4}$$

where

$C_w = (1.1 + 0.0536 \times U_{10}) \times 10^{-3}$, and U_{10} = Wind speed at 10 m height.

$$\tau_{bx} = \rho C_b (u^2 + v^2)^{1/2} u \tag{4.5}$$

$$\tau_{by} = \rho C_b (u^2 + v^2)^{1/2} v \tag{4.6}$$

where

$C_b = 2.3 \times 10^{-3}$

The following boundary conditions have been used: a) a radiation condition at the northern and southern boundaries normal to the coast (Orlanski, 1976); b) an adiabatic condition of no sea surface elevation at the offshore boundary located at the shelf break (Beardsley and Haidvogel, 1981); and c) normal flow equal to zero at the coastal boundary.

5. MODEL EXPERIMENTS

5.1. Numerical experiment using the cold front wind

The Finite Element grid of linear triangular elements for this region and used in the model is represented in figure 5. An integrating time step of 300

s is used in all experiments. In order to minimize effects of initialization, the model is forced for 24 h from rest, with a constant and uniform northeast wind of 5 m s^{-1}. A time ramp of 2 h is also used to bring the wind speed from zero to its 5 m s^{-1} value at the beginning of the integration. After the initial 24 h «warming up» of the model, the conceptual model of the cold front is then used to simulate the passage of a cold front, wich requires about two days time. After this step, a constant 5 m s^{-1} wind field is integrated for one more day.

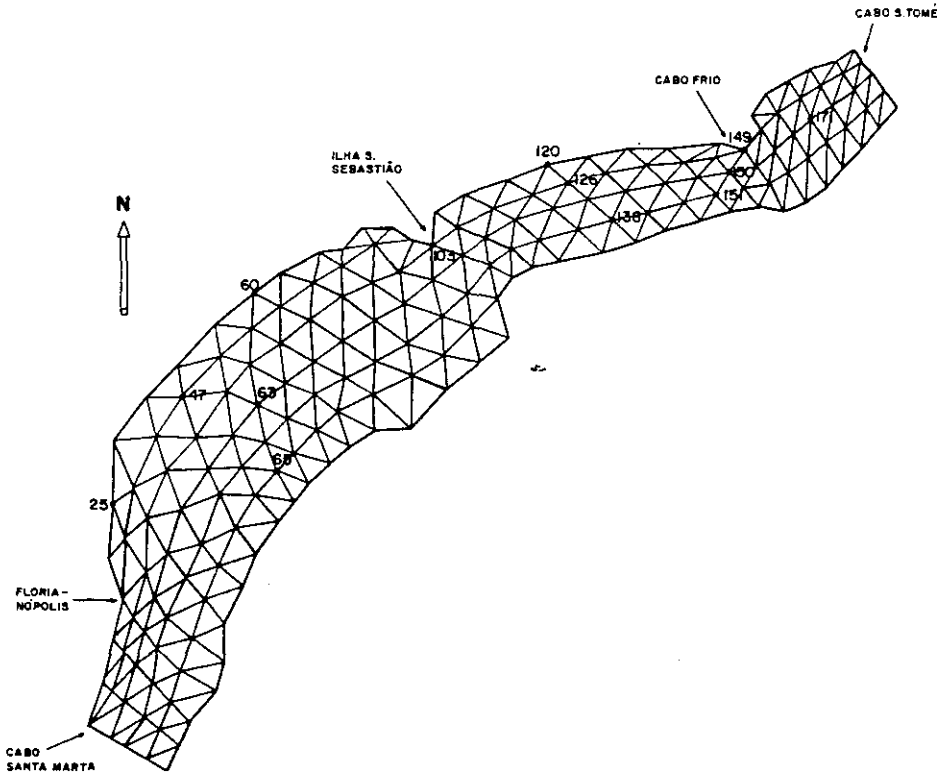

Figure 5.—Finite Element grid for the South Brazilian Bight. Number of nodes = 299 and number of elements = 188.

5.1.1. **Momentum balance**

With the current velocities and sea surface anomalies generated by the model, plus the wind stress forcing, time series of each term of the equations of momentum were generated for analysis. In figures 6, 7 and 8, these time series are plotted for the grid nodes 47, 63 and 65 (fig. 5), located on the 25, 77 and 127 m isobaths, respectively.

As expected, the momentum balance for the direction normal to coast is highly dominated by a geostrophic balance between the across-shelf pressure gradient and the Coriolis terms. The passage of the front introduces a cross-

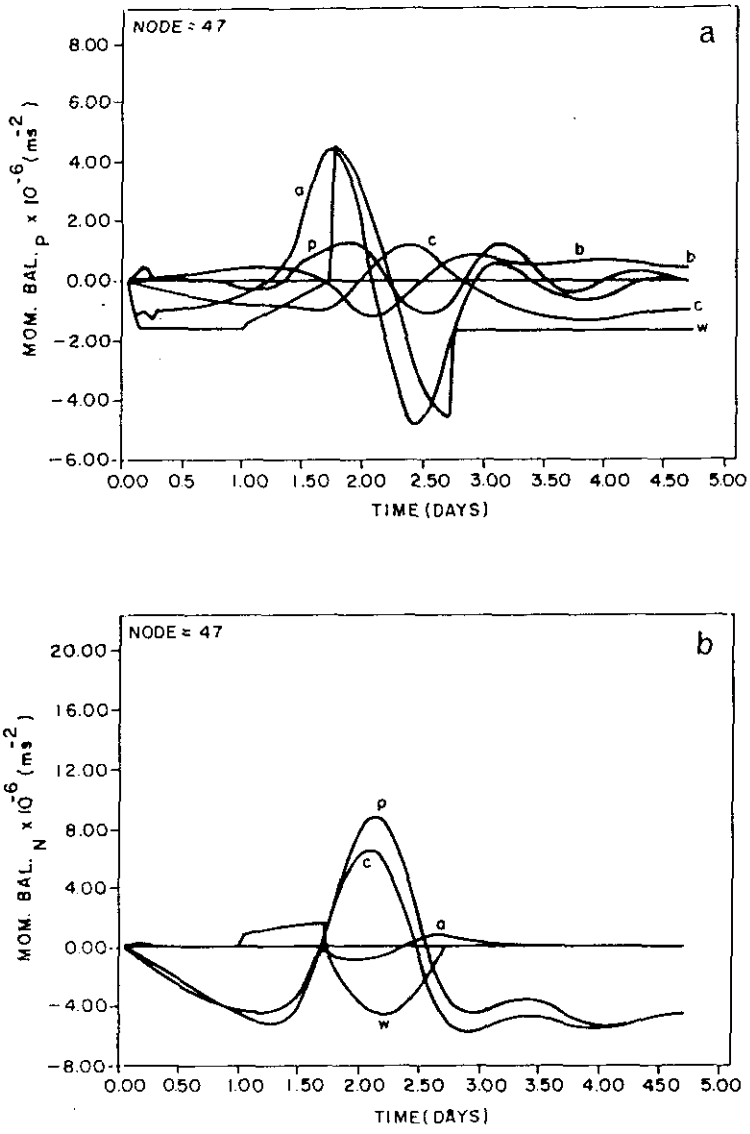

Figure 6.—Alongshelf (a) and cross-shelf (b) momentum balances at node 47 (fig. 5) for the cold front experiment. Units are m s^{-2}. a = local acceleration term, c = Coriolis term (—fv and + fu for the cross-shelf and alongshelf directions), p = pressure gradient term, w = wind stress term, b = bottom stress.

shelf acceleration on the flow which is almost balanced by the wind stress itself. Even during the passage of the front, the pressure gradient and Coriolis acceleration fields are seen to act together, preserving most of the geostrophic characteristic of the flow.

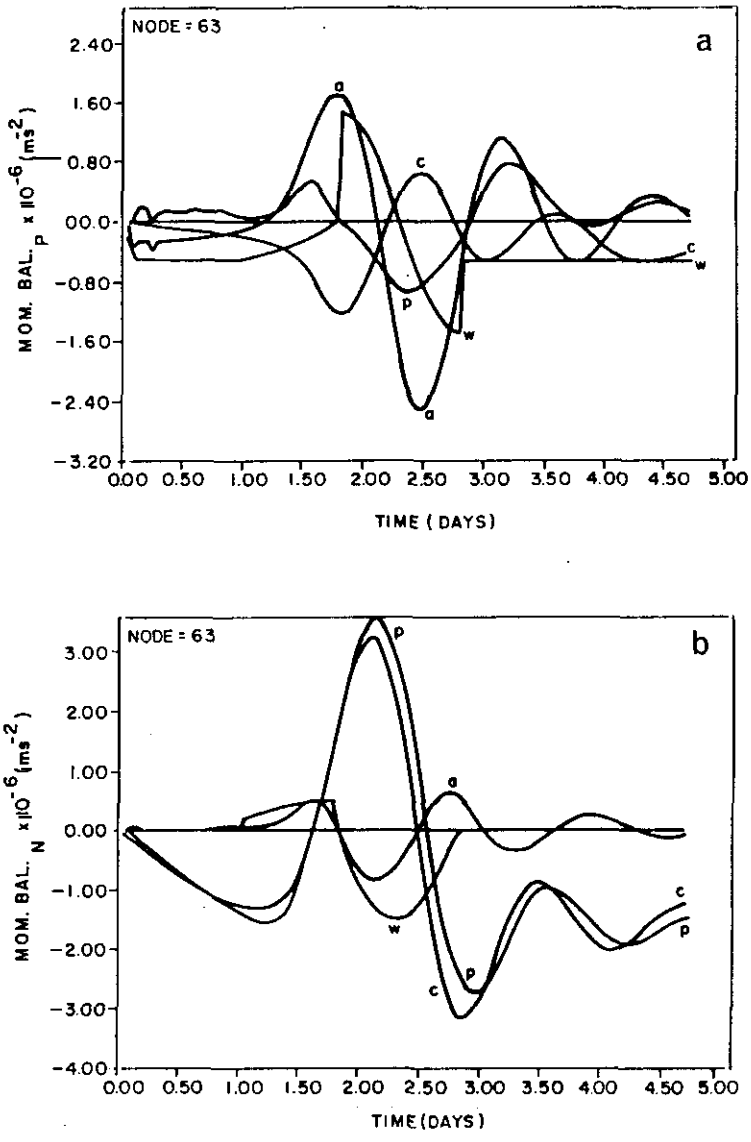

Figure 7.—As in figure 6 except at node 63.

The momentum balance for the longshore direction is more complex. For the steady state condition of a relatively constant wind blowing for a couple of days, the main balance for the deeper nodes is between the wind stress and the Coriolis term (Ekman balance), plus some contribution of the alongshore pressure gradient. As the coast is approached and the water gets shallower,

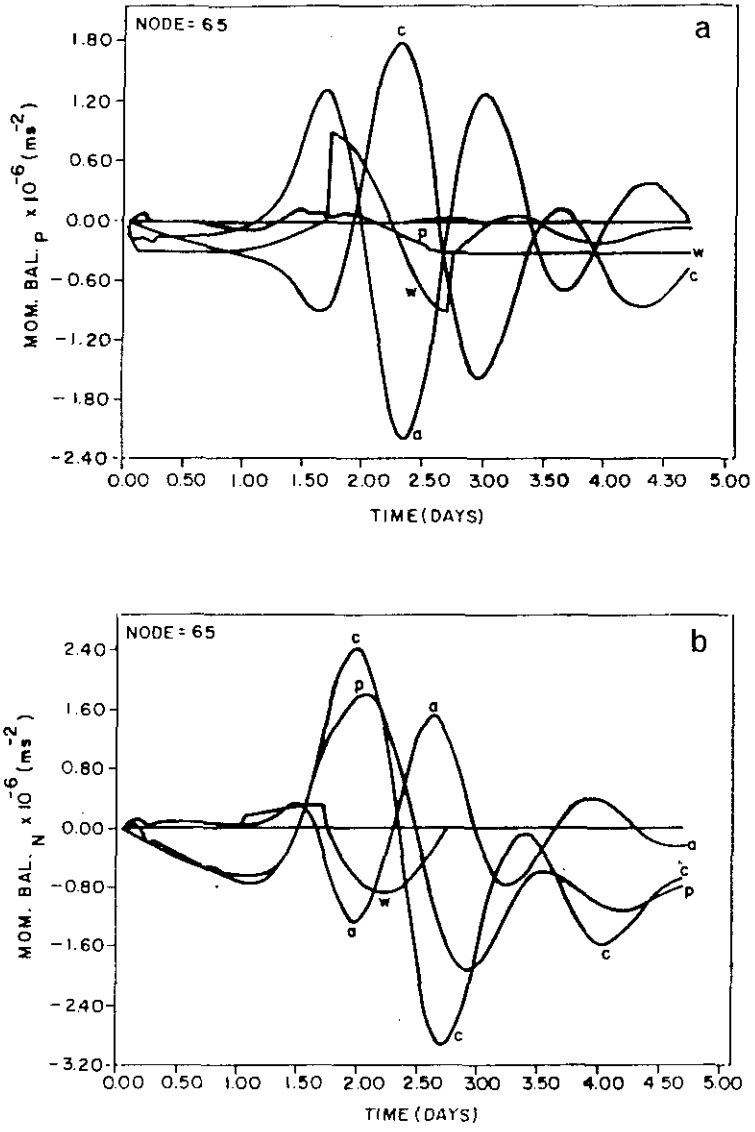

Figure 8. As in figure 6 except at node 65.

the bottom friction increases, tending to balance the wind stress for the inner shelf. For a more realistic time dependent situation, these results show that the passage of the front induces a large alongshore acceleration in the flow; this results in the generation of inertial period waves after the wind returns to its steady state. The decaying time scale of these oscillations is directly proportional to the water depth, and seems to be on the order of two days for the outer shelf, and one day for the inner shelf.

The time mean of each term in the momentum equations for different nodes and for the entire period of simulation is presented in Tables III and IV. The mean value of the terms confirm the analysis derived from the time series figures.

TABLE III

Time mean of the cross-shelf momentum equation terms ($\times 10^{-7}$ m s^{-2}).

Terms / *Nodes (depth)*	*Local accel.*	*Advec.*	*Coriolis*	*Press. Grad.*	*Wind Stress*	*Bottom Stress*	*Eddy Visc.*
47 (25)	0.33	0.22	—27.68	—21.12	—4.00	—0.58	—0.10
63 (77)	0.12	0.05	— 7.70	— 6.70	—1.26	—0.05	—0.02
126 (50)	—0.04	0.23	—42.00	—39.70	—1.57	—0.16	0.23
138 (123)	—0.48	0.11	—17.58	—17.85	0.49	—0.02	0.03
150 (117)	0.08	—0.13	—32.60	—33.04	1.48	—0.15	0.10
151 (136)	0.52	0.60	—26.52	—26.15	0.70	—0.45	—0.45

TABLE IV

Time mean of the alongshelf momentum equation terms ($\times 10^{-7}$ m s^{-2}).

Terms / *Nodes (depth)*	*Local accel.*	*Advec.*	*Coriolis*	*Press. Grad.*	*Wind Stress*	*Bottom Stress*	*Eddy Visc.*
47 (25)	—1.63	0.22	—5.37	1.16	—11.78	2.91	0.13
63 (77)	—0.44	0.03	—2.57	0.55	— 3.73	0.09	—0.10
126 (50)	—3.18	0.06	—5.17	—7.31	— 5.89	4.12	0.37
138 (123)	—0.91	0.04	—0.85	—0.21	— 2.10	0.42	0.11
150 (117)	—1.67	0.05	—5.18	—5.69	— 2.13	1.29	—0.41
151 (136)	—1.47	0.24	—1.42	—1.63	— 2.14	0.81	—0.01

5.1.2. **Vorticity balance**

In order to get a better understanding of how the vorticity is being distributed and balanced in the system, the model results and the wind stress

forcing were used to calculate, at each time step, the terms of the barotropic vorticity equation below (Csanady, 1981);

$$\underset{a}{\frac{\partial \zeta}{\partial t}} + u\underset{a_x}{\frac{\partial \zeta}{\partial x}} + v\underset{a_y}{\frac{\partial \zeta}{\partial y}} - f\frac{\partial \eta}{\partial t} = -g\left(\underset{c}{\frac{\partial H}{\partial x}\frac{\partial \eta}{\partial y}} - \underset{j}{\frac{\partial H}{\partial y}\frac{\partial \eta}{\partial x}}\right) +$$

$$\underset{w}{\left(\frac{\partial \tau_{xs}}{\partial x} - \frac{\partial \tau_{ys}}{\partial y}\right)} - \underset{b}{\left(\frac{\partial \tau_{xb}}{\partial x} - \frac{\partial \tau_{yb}}{\partial y}\right)} \qquad (5.1)$$

where $\zeta = \partial q_y/\partial x - \partial q_x/\partial y$.

Figures 9, 10 and 11 show the time series plots of every term in Eq. (5.1) for differents nodes.

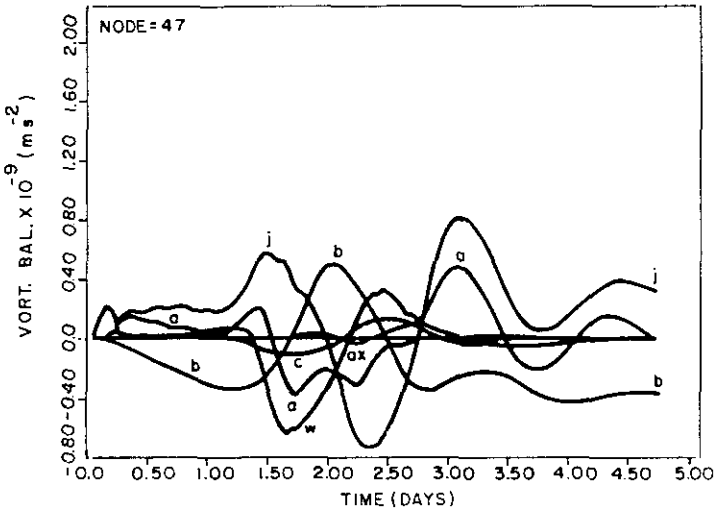

Figure 9.—Vorticity balance at node 47 for the cold front experiment. Units are m s^{-2}. a = local rate of change, J = Jacobian, w = wind curl, b = bottom stress curl, a_x and a_y advectives terms.

The most conspicuous feature in these plots is that the vorticity is seen to be mostly generated by the topographic term (Jacobian), that is, by the stretching of the vortex filaments by the geostrophic flow crossing the isobaths. Even during the passage of the front at the grid point of interest, when the vorticicty of the wind increases, a direct transfer of wind vorticity to the system seems to be only a secondary mechanism of vorticity generation within the flow. For the shallow region near the coast, these results indicate

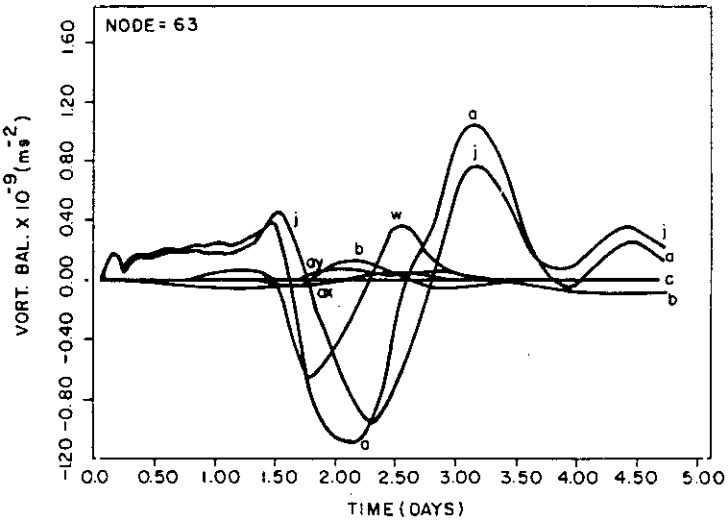

Figure 10.—As in figure 9 except at node 63.

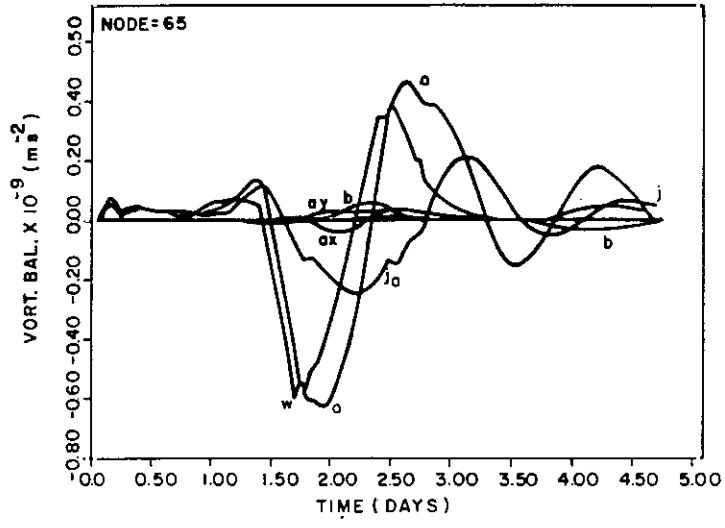

Figure 11.—As in figure 9 except at node 65.

that the bottom friction vorticity is a very efficient mechanism for removing vorticity generated by topographic stretching. Therefore, for the inner shelf, a balance between the topographic vorticity and bottom friction vorticity dominates the flow. For the mid and outer shelf, with only a minor

contribution from the bottom friction vorticity sink, the topographic vorticity is observed to generate a large local time rate of change of vorticity in the flow. The passage of the front introduces an oscillation in the vorticity field which a long time decay.

5.2. Numerical experiment using the coastal wind

The main objective of this section is to analyse the barotropic response of the shelf waters to a forcing field derived from the observed coastal wind. At 6 hours intervals, the observed winds at the coastal stations are used to update the wind stress at every grid point. The interpolation method used is described in Allender (1974). The period chosen for the simulation was July 18-29, 1984, due to its being the only period for which a complete data set (winds, sea level and barometric pressure) was available. During this period a cold front was observed and it propagated throughout the region with a velocity of aproximately 1.000 km day^{-1}. This velocity is twice the mean velocity determined from the analysis of satellite images.

The same numerical grid, boundary conditions and physical parameters used in the previous experiment were utilized in this second experiment. In order to minimize the initialization problem and to obtain a better dynamic adjustment, the model was integrated for 29 hours, utilizing the wind forcing from 0 h on July 18, 1984, with a ramp of 12 hours. In the 30th hour of integration, the wind was updated to the wind corresponding to the 6 hours on July 18, 1984.

5.2.1. Coastal sea level

Figure 12 shows the time series of sea surface elevation anomalies predicted by the model and observed in the coastal stations for the period considered. Also shown in figure 12 are the maximum values of the cross-correlation between these two variables and the coresponding phase lag.

It can be observed that the maximun correlation grows monotonically from South to North, varying from $r = 0.76$ at Imbituba station to $r = 0.82$ at Rio de Janeiro, with the phase lag increasing from 0 to 3 hours. The northward improvement of the model in simulating the sea level anomalies can be related to the idea that at a particular point, the sea level anomaly depends not only on the local wind, but also on the remote forcing induced by the winds to the south (for this region) through the propagation of shelf wave signals. Therefore, if this interpretation is correct, the simulated sea level at the southerm stations would not be receiving all the remote wave energy further to the south. due to the truncated model domain.

It might be noted that the model simulated most of the sea level variation patterns whereas it underestimated the crest and troughs. It is speculated that this tendency for a reduced variance present in the simulations is related to

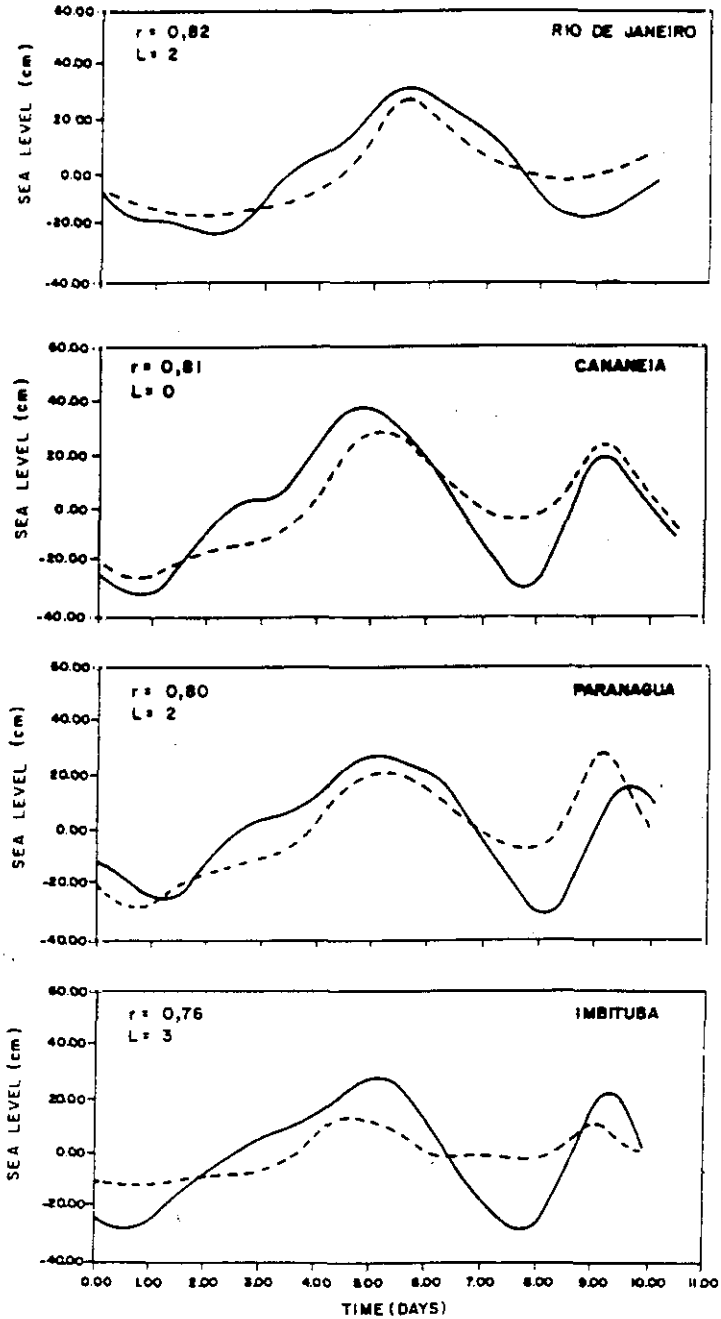

Figure 12. Coastal sea level anomalies modeled (broken line) and observed (solid line) for the coastal wind experiment.

the quality of the wind data. Although the full dynamic relation between the wind and the sea level may be complex, the positive (negative) coastal sea level anomalies can be generally related to the onshore (offshore) Ekman transport induced by alongshore southerly (northerly) winds.

Inspection of figure 12 indicates a northward propagation of the sea level anomalies. The estimated speed of this propagation, on the order of 1.150 km day^{-1}, has been obtained in the following way: the cross-correlation between the sea level anomalies at a reference coastal grid point (near Imbituba station) and the anomalies at all other coastal grid points was calculated. Next, the lag corresponding to the maximum correlation was plotted against distance between each two grid points. The slope of the linear fit through these points gives the average speed of propagation.

In order to compare the above speed of propagation with the speed of free continental shelf waves, the Brink *et al.* (1984) model was used to calculate the dispersion relation of the barotropic mode for three transversal sections (Santa Marta, Cananéia and Cabo Frio). For the Santa Marta section and for a long wave with a period of 6 days (the forcing period), a phase velocity of 450 km day^{-1} and a wavelength of approximately 2.700 km are observed. For the Cananéia section and the same period, the phase velocity and the wavelength are 650 km day^{-1} and 3.900 km, respectively. For the Cabo Frio section, the phase velocity is 290 km day^{-1} and the wavelength is 1.745 km.

The model results and the observations pointed out that the coastal sea level contains perturbations. These perturbations propagate to the north with a phase velocity of aproximately 1.000 km day^{-1}, the speed of propagation of the cold front present during the simulated period. Therefore, it seems that for this case, the sea level anomalies propagate in phase with the wind forcing, with only a secondary contribution from remote forcing due to free long waves.

6. DISCUSSION AND CONCLUSIONS

The results obtained with the barotropic model indicate that the main mechanisms governing the winter time dynamics of this region can be described by the following set of momentum and vorticity equations:

$$fq_y = gH\frac{\partial \eta}{\partial x} \tag{6.1}$$

$$\frac{\partial q_x}{\partial t} + \varepsilon\frac{\partial v q_x}{\partial y} + fq_x = -gH\frac{\partial \eta}{\partial y} + \frac{1}{\partial}(\tau_{ys} - \delta\tau_{yb}) \tag{6.2}$$

$$\frac{\partial \zeta}{\partial t} + \varepsilon v\frac{\partial \zeta}{\partial y} = -g\left(\frac{\partial H}{\partial x}\frac{\partial \eta}{\partial y} - \frac{\partial H}{\partial y}\frac{\partial \eta}{\partial x}\right) + \mathrm{curl}_k\,\tau_s - \psi\,\mathrm{curl}_k\,\tau_b \tag{6.3}$$

where $\delta = 1$ only near the shelf break; otherwise $= 0$

$\varepsilon = 1$ only near Cabo Frio; otherwise $= 0$

$\psi = 1$ only in the inner and mid shelf; otherwise $= 0$

These results indicate that the main momentum balance is very similar to that presented in most analytical models for wind forced continental shelf waves (e.g., Gill and Schumann, 1974). Therefore, non-local effects produced by the propagation of long waves should not be neglected. In other words, a part of the sub-tidal changes in sea level and current variability at a specific point of this region cannot be explained with local winds only.

It should be noted that the typical speed of propagation of cold fronts in the region is of the same order of magnitude as for continental shelf wave propagation, i.e., 500 km day^{-1}. The case studied in Section 5.2.1. is a possible but not a common occurence. In the central part of the domain, where the shelf width widens, the free waves signal can propagate faster than the front, indicating the importance of remote forcing in this area.

For the inner and mid-shelf regions, where the non-local effects are important, the vorticity balance analysis shows that the main mechanism for vorticity generation is the topographic stretching with contributions from bottom friction vorticity for the shallow nodes and local vorticity changes for the mid-shelf region. Similarly to the dynamics of shelf waves, wind vorticity does not seem important for these regions. For the outer shelf, where the Ekman dynamics seem to dominate the flow, wind vorticity is seen to be of importance, especially during the passage of cold fronts.

It is evident from figures 6, 7 and 8 (and others not presented here) that the passage of a front generates a strong inertial signal. Also, the magnitude of this signal increases as the water depth increases. As may be inferred from figure 4, the passage of a frontal system introduces a rotation in the wind vector, which is in the same direction of rotation expected for an inertial motion in the southern hemisphere, i.e., counterclockwise. Also, figure 4 shows that for a winter time frontal system at the SBB, the wind goes through a complete turn in 750 km. With a velocity of 500 km day^{-1}, this gives a 1.5 day period for a complete wind rotation; or an angular frequency of $\omega = 2\pi / T = 0.49 \times 10^{-4}\ s^{-1}$, which is very near the inertial frequency of the system at this latitude, $f = -0.62 \times 10^{-4}\ s^{-1}$. It seems, therefore, quite natural to speculate on the role of a resonance mechanism between the wind and the inertial mode of the system.

Consider the vertically integrated, linearized momentum equations, with the pressure gradient term neglected and the bottom friction parameterized to be linearly proportional to the mean water velocity. The following set of equations result;

$$\frac{\partial u}{\partial t} - fv = \frac{\tau_{xs}}{\rho H} - \frac{ru}{\rho H} \tag{6.4}$$

$$\frac{\partial v}{\partial t} + fu = \frac{\tau_{ys}}{\rho H} - \frac{rv}{\rho H} \tag{6.5}$$

Multiplying Eq. (6.5) by $i=(-1)^{1/2}$ and adding to Eq. (6.4) we get

$$\frac{\partial V}{\partial t}+ifV+\frac{r}{H}V=\frac{T(t)}{\rho H} \tag{6.6}$$

where

$V=u+iv$ is the vertical mean velocity of the water column

$T=\tau_x+i\tau_y$ is the wind stress vector

r = bottom friction coefficient

H = water depth

Taking $T=Ae^{i\omega t}$ and assuming $V=v_o e^{i\omega t}$, the solution of the Eq. (6.6) is:

$$V(t)=\frac{(A/\rho H)}{((\omega+f)^2+(r/H)^2)^{1/2}}e^{i(\omega t+B)} \tag{6.7}$$

where

$$B=\frac{\pi}{2}-\tan^{-1}\left(\frac{(r/H)}{\omega+f}\right)$$

This solution shows that resonance can occur if $\omega+f\cong 0$ and the bottom friction is small. The $(\omega+f)$ term will only tend to zero for the southern hemisphere ($f<0$) if $\omega>0$, a situation of counterclockwise rotation of the wind, and $|\omega|\cong|f|$. An estimate of the magnitude of the water velocity as given by Eq. (6.7) for different values of f and for typical values of bottom stress obtained from the momentum balance presented in Section 5.1.1 is given in Table V.

TABLE V

Terms of Eq. 6.7 calculated using typical values generated by the model and for different forcing conditions. A wind frequency $\omega=0.49\times10^{-4}$ s^{-1} is used in columns 5, 6 and 8.

H (cm)	v cm s^{-1}	τ_{xh}/ρ	r	$\lvert v(t)\rvert$ $f<0$	$\lvert v(t)\rvert$ $f>0$	$\lvert v(t)\rvert$ $f<0, \omega=0$	B
2500	10.0	2.3×10^{-1}	2.3×10^{-2}	12.6	1.8	3.2	55°
7700	5.0	5.8×10^{-2}	1.2×10^{-2}	5.0	0.6	1.1	81°
12500	3.5	2.8×10^{-2}	8.0×10^{-3}	3.0	0.4	0.7	87°

The column 5 of Table V shows that the velocity values obtained by the resonance theory compare very well with the model results (column 2). The column 6 shows very small velocity values for the same forcing but for the

northern hemisphere. The column 7 gives the theoretical values for southern hemisphere with a stationary wind. Again, the predicted values are substantially smaller than those given by the model. Therefore, it seems quite possible that the resonance might be present, given the small difference between the wind frequency and the inertial mode. It is interesting to note the reduction of the phase lag between the wind and the current, with the increase of the bottom stress as the coast is approached (last column in Table V). This solution indicates that near the coast, a balance between the wind and the bottom stress might dominate with the current flowing in the direction of the wind with almost no phase lag. For the outer shelf, the solution indicates a phase lag of 90° which is a typical value of an Ekman balance. Both results agree with the previous analysis of the momentum balance.

It should also be realized that some care must be exercised with regard to the results presented for the region near the shelf break, since in this region the Brazil Current plays an important role in the circulation, with an associated baroclinic field of mass, not accounted for in the model (Castro Filho *et al.*, 1987 and Garfield, 1990).

Finally, the parameterization of the bottom stress of the model uses the mean velocity in the water column. It is known that the velocity near the bottom differs from the mean velocity in magnitude and direction. Therefore, an implementation of a bottom stress that would take this fact into account should lead to a more realistic representation of the actual dynamics. Although, current meter data were not available for comparison with model results, the reasonable agreement of sea level computed by the model, as compared to observations, indicates that most of the dynamics of the region are well represented by this simple model.

Acknowledgements

The authors wish to thank the Interministerial Comission for Marine Research (CIRM), Brazil, for the support of the Project DINACO (nº 9298) through which this paper was prepared; José Carlos Rodrigues of INPE for help in the development of the Cold Front Conceptual Model; Rogério Bertolossi of Brazilian Air Force for help in the analysis of the satellite images; Drs. Merritt R. Stevenson and Yellisety Viswanadham of INPE for discussing and improving the manuscript.

REFERENCES

Allender, H. A. (1977): Comparison of Model and Observed Currents in Lake Michigan *J. Phys Oceanogr.* 7, 711-718.

Beardsley, R. C. and D. B. Haidvogel (1981): Model Studies of Wind-Driven Transient Circulation in the Middle Atlantic Bight. I. Adiabatic Boundary Condition. *J. Phys Oceanogr.* **11**, 355-375.

Brink, K. H. and D. C. Chapman (1987): Programs for Computing Properties of Coastal-Trapped Waves and Wind-Driven Motions over The Continental Shelf and Slope.

Technical Report Nº WHOI-87-24. Second Edition. Woods Hole Oceanographic Institution. Woods Hole, Massachussetts 02543.

Castro Filho, B. M. (1985): Subtidal Response to Wind Forcing in the South Brazil Bight During Winter. Ph. D. Dissertation. Rosenstiel School of Marine and Atmospheric Science, University of Miami. Miami, Florida.

Castro Filho, B. M., L. B. de Miranda e S. Y. Miyao (1987): Condições Hidrográficas na Plataforma Continental ao Largo de Ubatuba: Variações Sazonais e em Média Escala. *Bolm. Inst. Oceanogr.*, S. Paulo, **35,** 135-151.

Csanady, G. T. (1984): Circulation in the Coastal Ocean. *D. Reidel Publishing Co,* 279 p.

Garfield III, N. (1990): The Brazil Current at Subtropical Latitudes. Ph.D. Dissertation. *University of Rhode Island.* 122 p.

Gill, A. E. and E. H. Shumann (1974): The generation of Long Shelf Waves by the Wind. *J. Phys Oceanogr* **4,** 83-90.

Hasse, L. (1974): A Note on the Surface-to-Geostrophic Wind Relationship from Observations in the German Bight. Bound. Layer Meteor., **6,** 197-201.

Jenkins, G. M. and D. G. Watts (1968): Spectral Analysis and its Applications. Holden Day, San Francisco, 525 p.

Kourafalou, V., J. D. Wang and T. N. Lee (1984): Circulation on the Continental Shelf of the Southeastern United States. Part III: Modeling the Winter Wind-Driven Flow. *J. Phys. Oceanogr.* **14,** 1022-1031.

Kundu, P. K. (1976): Ekman Veering Observed Near the Ocean Bottom. *J. Phys. Oceanogr.* **6,** 238-242.

Leendertse, J. J. and S. K. Liu (1975): A Three-Dimensional model for Estuaries and Coastal Seas. Vol. II, Aspects of Computation, R-1764-OWRT. The Rand Corporation.

Lorenzzetti, J. A., J. D. Wang and T. N. Lee (1988): Two-Layer Model of Summer Circulation on the Southeast U.S. Continental Shelf. *J. Phys. Oceanogr.* **18,** 591-668.

Matsuura, Y. (1983): Estudo Comparativo das Fases Iniciais do Ciclo de Vida da Sardinha-Cascuda, Harengula Jaguana (Pisces. Clupeidae) e Nota sobre a Dinamica da População da Sardinha-Verdadeira na Região Sudeste do Brasil. Dissertação de Livre-Docência. *Instituto Oceanográfico, Universidade de São Paulo,* 150 p.

Miranda, L. B. de (1982): Análise de Massas de A'gua da Plataforma Continental e da Região Oceânica Adjacente: Cabo de São Tomé (RJ) a Ilha de São Sebastião (SP). Dissertação de Livre-Docência». *Instituto Oceanográfico, Universidade de São Paulo,* 123 p.

Orlanski, I. (1976): A simple Boundary Condition for Unbounded Hyperbolic Flows. *J. Comp. Phys.* **21,** 251-269.

Signorini, S. R. (1979): A Three-Dimensional, Finite Element Numeric Model of Circulation and Diffusion-Advection Processes for Estuarine and Coastal Application (with Application to Bay of Ilha Grande, Brazil). Ph. D. Dissertation, University of Rhode Island.

Wang. J. D. and J. J. Connor (1975): Mathematical Modeling of Near Coastal Circulation. R.M. Parsons Laboratory, Technical Report 200, Massachussets Institute of Technology, Cambridge, Mass.

Walters, R. A. and C. Heston (1982): Removing Tidal-Period Variations from Time-Series Data Using Low-Pass Digital Filters. *J. Phys. Oceanogr.* **12,** 112-115.